Break-up reactions of 6Li, 7Be, and 8B

T. Issatayev
Joint Institute for Nuclear Research ,Russian Federation

S. M. Lukyanov
Joint Institute for Nuclear Research ,Russian Federation

Yu. M. Sereda
Joint Institute for Nuclear Research ,Russian Federation

A. G. Artukh
Joint Institute for Nuclear Research ,Russian Federation

D. Aznabayev
Joint Institute for Nuclear Research ,Russian Federation

See next page for additional authors

Break-up reactions of 6Li, 7Be, and 8B

Authors

T. Issatayev, S. M. Lukyanov, Yu. M. Sereda, A. G. Artukh, D. Aznabayev, C. Borcea, S. Calinescu, B. Erdemchimeg, B. M. Hue, A. M. Kabyshev, S. A. Klygin, G. A. Kononenko, K. A. Kuterbekov, K. Mendibayev, V. V. Ostashko, Yu. E. Penionzhkevich, F. Rotaru, T. D. Thiep, and A. N. Vorontsov

Break-up reactions of ^{6}Li, ^{7}Be and ^{8}B

T. Issatayev[*,1,2,3], S.M. Lukyanov[1], Yu.M. Sereda[1],
A.G. Artukh[1], D. Aznabayev[1,2], C. Borcea[4],
S. Calinescu[4], B. Erdemchimeg[1], B.M. Hue[1,5],
A.M. Kabyshev[3], S.A. Klygin[1], G.A. Kononenko[1],
K.A. Kuterbekov[3], K. Mendibayev[1,2,3], V.V. Ostashko[6],
Yu.E. Penionzhkevich[1,7], F. Rotaru[4], T.D. Thiep[5], A.N. Vorontsov[1],

[1]Joint Institute for Nuclear Research, Dubna, Russia

[2]Institute of Nuclear Physics, Almaty, Kazakhstan

[3]L.N. Gumilyov Eurasian National University, Nur-Sultan, Kazakhstan

[4]National Institute for Physics and Nuclear Engineering, Bucharest Magurele, Romania

[5]Institute of Physics, VAST, Hanoi, Vietnam

[6]Nuclear Physics Institute, Kyev, Ukraine

[7]National Research Nuclear University "MEPhI", Moscow, Russia

E-mail: issatayev@jinr.ru

Secondary beams (^{6}Li, ^{7}Be, ^{8}B) were obtained by the separation of fragmentation products of a ^{15}N ion beam (50 MeV/A) impinging on a Be target using the COMBAS spectrometer. The secondary products were detected by a telescope consisting of five Si-detectors (dE) and a stop CsI(Tl) detector. The telescope allowed us to achieve unambiguous particle identification of fragments originating from incident secondary beams as well as their reaction products resulting from interaction with the Si detectors, chosen as a secondary target. This way, break-up reactions of ^{6}Li, ^{7}Be and ^{8}B have been studied in this experiment, in particular the longitudinal momentum distributions of ^{7}Be fragments in the break-up of ^{8}B on a Si have been measured at 30 MeV/A.

Introduction

In recent years, the study of nuclear reactions induced by loosely bound light nuclei has attracted intensive experimental and theoretical attention. The experimental investigations of clustering nuclei and halo-like nuclei have been developed quite strongly with the aid of both radioactive ion beams (RIBs) and beams of stable loosely bound nuclei [1]. Using neutron-rich light radioactive projectiles of He, Li and Be impinging on various reaction targets measurements of the interaction cross section and of the nuclear radii were performed leading to the discovery of the neutron halo [2]. Since then, the existence of neutron halos has been confirmed for some other nuclei. Soon after, total reaction cross section and neutron-removal cross section (σ_{-xn}) have been measured for ^{6,8}He and $^{6-9,11}$Li nuclei using silicon detectors as active target [3]. On the other hand, the proton halo is more diffucult to pindown due to the presence of the Coulomb barrier. The proton drip-line nucleus ^{8}B emerges as one of the best candidates for a proton-halo nucleus: the valence proton is in a p-state and low separation energy is 137 keV. So far, proton-halo structure of ^{8}B has been under debate from the first experimental observation of its unusual behavior via the measurement of its quadrupole moment [4]. Moreover, theoretical calculation indicated that the result could also be explained by cluster effects [5]. Furthermore, even if the measurement at low energies (20 and 60 MeV/A) showed large total cross sections indicating the existence of a proton halo in ^{8}B [6], the results deviated considerably from other experiment at higher energy (790 MeV/A) [7]. Another evidence in favour of halo was the measurement of the longitudinal momentum distribution of ^{7}Be via one proton removal channel of ^{8}B [8, 9]. This experiments showed a much narrower distribution than the one for stable nuclei. However, only a small radius enhancement was observed in the the quasi-elastic scattering of ^{8}B at 40 MeV/A [10].

Thus, from the experimental point of view, proton halo structure of ^{8}B is still an open question. Although the theoretical publications can explain the existence of a halo, exclusive experimental data including high-precision proton-removal cross section (σ_{-xp}) and momentum distribution are needed to support these theoretical approaches. The current study aims at a direct measurement of σ_{-xp} and break-up cross section (σ_{BU}) of ^{8}B and its neighboring loosely bound cluster nuclei (^{6}Li and ^{7}Be) respectively as well as momentum distribution of the break-up products.

The experimental set-up

In present experiment, the secondary cocktail beam was produced by fragmentation of ^{15}N beam (50 MeV/A) bombarding a Be target. Fragmentation products were separated and purified by the achromatic magnetic spectrometer COMBAS [11] (see Figure 1).

The energy dispersion was limited to less than 1% FWHM by analyzing slits. Two experimental runs at different values of the magnetic rigidity Bρ settings were performed: one leading to nuclei rather close to stability line and another
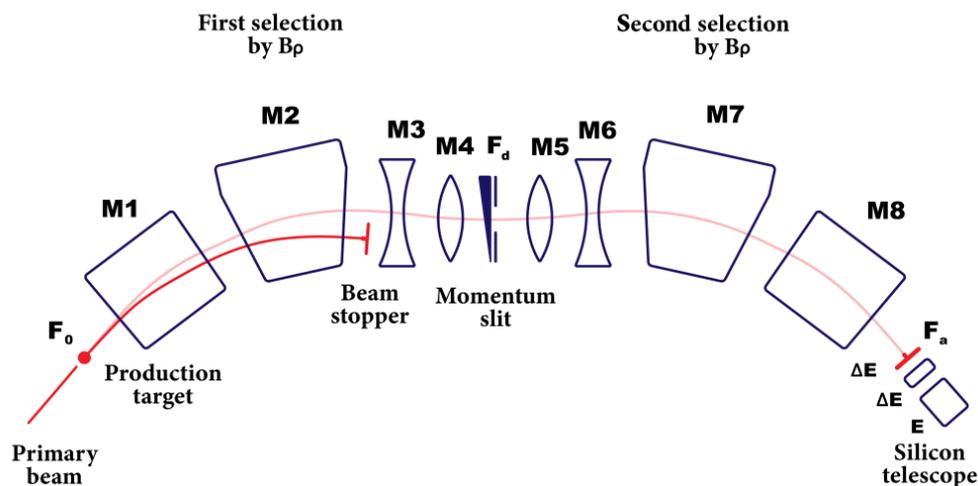
Figure 1. A schematic layout of the COMBAS spectrometer at JINR.

leading to proton rich nuclei.

The secondary products were detected by a telescope consisting of five Si-detectors and a CsI(Tl) detector used to measure the energy loss (dE) and the residual energy (E_r), respectively. The telescope was located in the focal plane of the COMBAS spectrometer and its scheme is shown Figure 2 (not to scale).
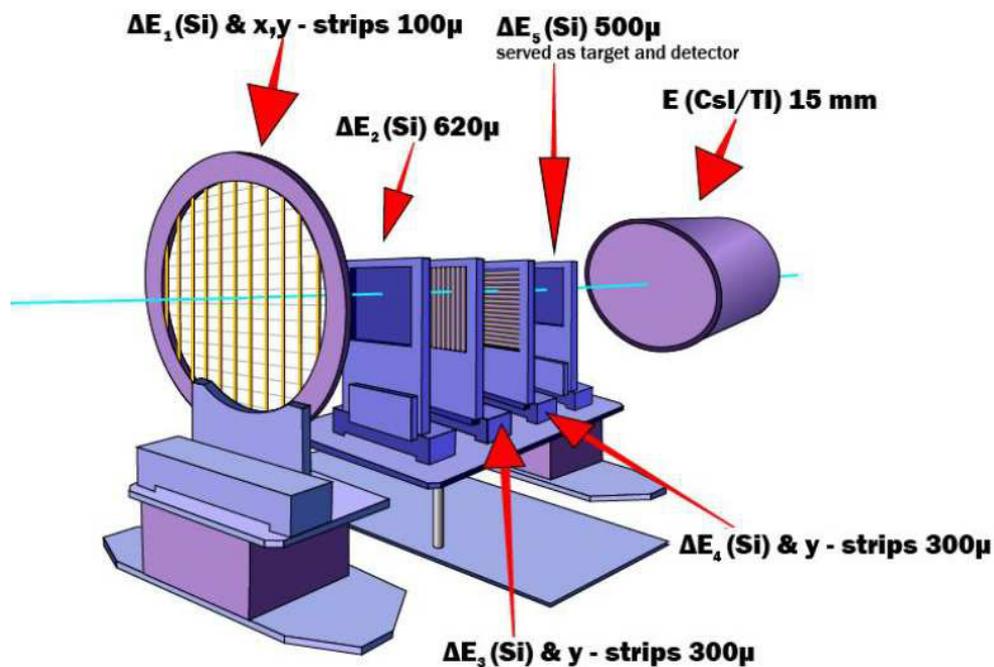

Figure 2. The telescope (not to scale) used in this experiment.

The first ΔE detector is a position sensitive Si detector ("x-y" double-sided strip detector). It was set not only for obtaining the ΔE information of the incoming secondary beam but also for triggering the data acquisition. This detector, was also used as the time of flight (TOF) start signal while the stop signal was provided by the cyclotron radio-frequency. Behind this detector, there were another single-pad Si (ΔE_2) and two other single-sided Si strip (ΔE_3 and ΔE_4) arranged horizontally and vertically respectively for both precise measurement of the spectra of the

secondary beams and control of beam divergence by measuring x-y coordinate distribution. The last Si detector, ΔE_5 (500 μm thickness, 50×50 mm^2) was employed for acquiring additional ΔE information and identification of reaction products in one of the upstream detectors. It was also used as a secondary target for the breakup cross section measurement. In order to measure the remaining energy of particles (E_r) a CsI(Tl) detector (15mm thickness, 200mm diameter) was used and mounted at the end of the telescope. Thus, the used telescope allowed us to obtain unambiguous particle identification both for incoming secondary beam and for the reaction products by using ΔE-TOF-E method.

Data analysis

To investigate the reactions induced by the secondary beams, a combination of all available information from detectors was used, including the Si detectors in front of ΔE_5 detector (target). The reaction products having the longest range were identified based on the information of energy loss in the ΔE_5 and E_r in the CsI(Tl) detector. The thickness of CsI(Tl) detector was sufficient to stop all of the reaction products. The two-dimensional ΔE_2-TOF matrix (Figure 3) is an example of the applied particle identification method. Multiple ΔE-TOF matrices were built for each of $\Delta E_1 \dots \Delta E_4$ detectors and for a chosen Bρ setting such as to identify unambiguously the reaction products. Figure 3 shows a typical identification spectrum ΔE_2-TOF taken with ΔE_2 for the first Bρ setting. In this figure we can see a clear separation of the following isotopes: ^{6}He, ^{7,8,9}Li, ^{10,11,12}Be and ^{13,14}B. From this cocktail of secondary beams shown in Figure 3, in the data processing a contour gate was set around each of the isotopes mentioned above.
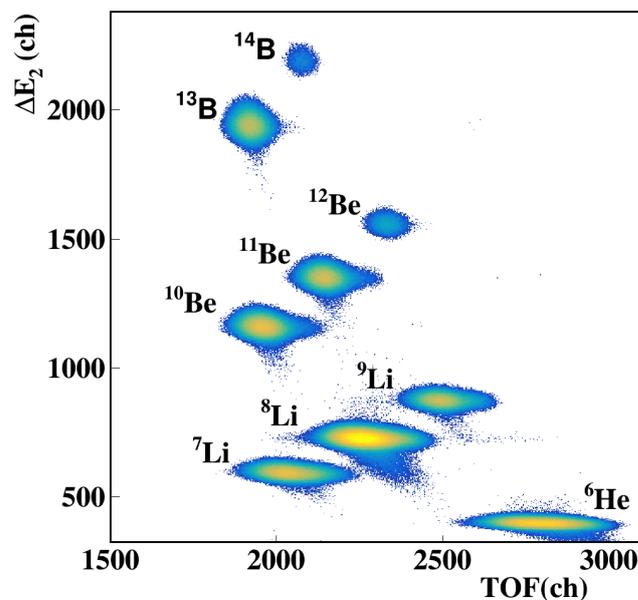

Figure 3. Yield vs. energy of ΔE_2 and TOF.

In the next step, the spectrum ΔE_5-ΔE_r (CsI) was built (Figure 4) from the cuts of ^{10}Be isotope in the spectra of previous detectors (ΔE_1-ΔE_4). Several regions can be obtained in this figure, which are marked correspondingly:
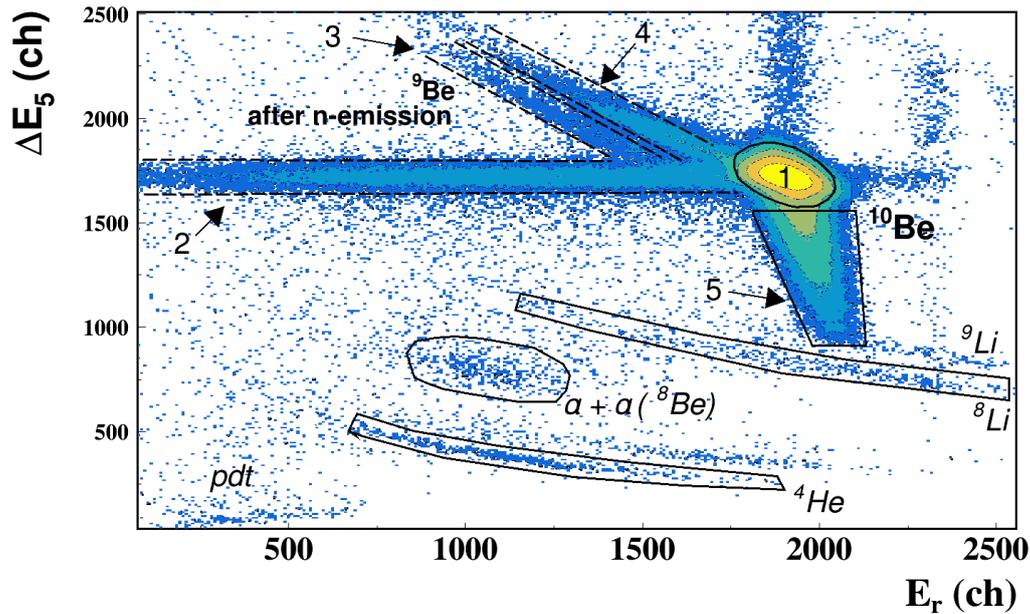
Figure 4. Yield vs. energy of ΔE_5 and E_r selected for 30 MeV/A ^{10}Be. (see explanation in the text).

- unreacted ^{10}Be events;

- reacted events inside the CsI(Tl) detector,

- ^{9}Be after one neutron-removal reaction from ^{10}Be;

- scattered events without changing atomic number (quasielastic events);

- channeling events in ΔE_5;

- Li after stripping one proton;

- $\alpha + \alpha$: events resulting from the decay of ^{8}Be nucleus produced after 2n emission from ^{10}Be (simultaneous detection of two α particles);

- pdt and ^{4,6}He obtained from the break-up of ^{10}Be into alphas and hydrogen isotopes.

The similar procedure was applied to the second Bρ setting, leading to production of ^{6}Li and for proton-rich nuclei as ^{7}Be and ^{8}B. Figure 5 shows measured yield versus energy loss ΔE_5 and ΔE_r, for secondary beams ^{4}He, ^{6}Li, ^{7}Be, ^{8}B. Areas corresponding non-reacted and reaction events on the Si are very well visible. A various range of reaction products mainly resulted from the break-up reaction of the selected isotopes was observed.

Results and discussion
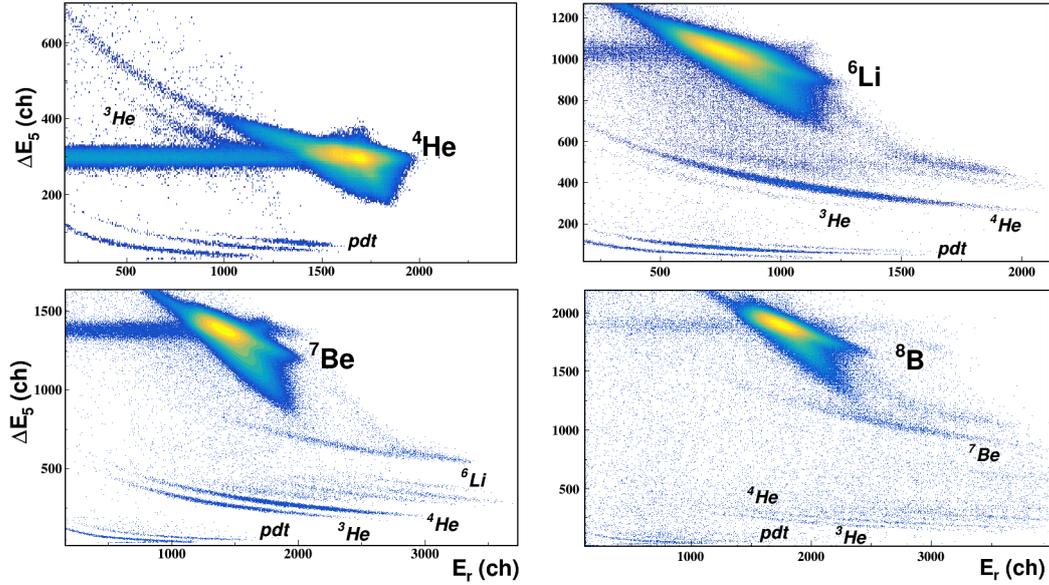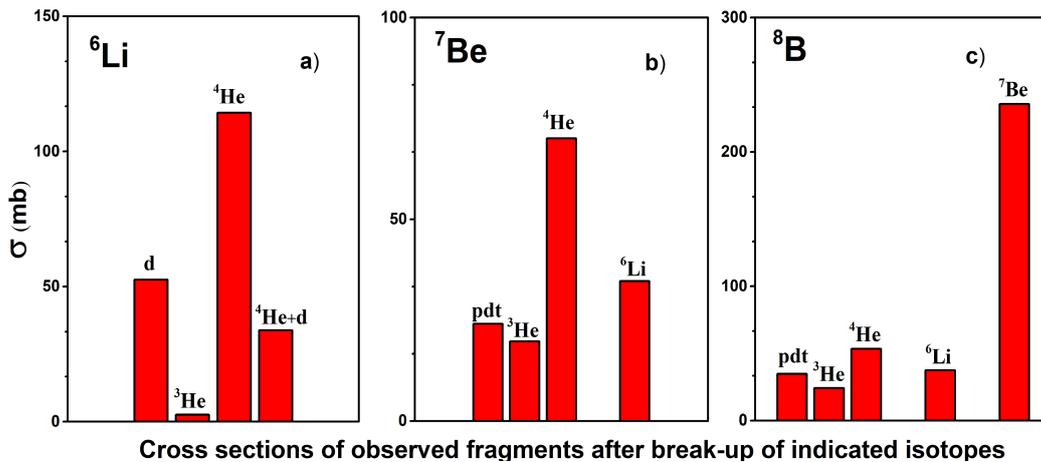
Break-up reaction cross section.

Figure 5. Measured yield vs. energy loss ΔE_5 and ΔE_r, for secondary beams ^{4}He, ^{6}Li, ^{7}Be, ^{8}B. Areas corresponding non-reacted and reactions on the Si are very well visible.

The break-up reaction cross-section for the channels indicated in the Figure 5 was calculated using the following formula:

$$\sigma_{BU_{channel}} = \frac{N_{select}}{N_{beam}N_{target}}$$ (1)

In this formula N_{select} is the number of events corresponding to the selected particle break-up channel, N_{beam} is the total number of non-reacted (selected isotope) events and N_{target} is the number of target particles/cm^2.

The breakup cross-sections for disintegration into charged fragments for ^{6}Li, ^{7}Be, ^{8}B nuclei were measured at energies: 18, 24, 30 MeV/A respectively (see Figure 6).

Figure 6. Measured break-up reaction cross section into various channels for ^{6}Li (a), ^{7}Be (b), ^{8}B (c) on Si at energies: 18, 24, 30 MeV/A respectively.

Figure 6 (a) illustrates that ^{6}Li mostly breaks into ^{4}He and d. This break-up probability is correlated to the separation energy: indeed ^{4}He or d separation is 1.47 MeV and break up probability into ^{3}He is much less due to very high value

of its separation energy (15.8 MeV). The obtained breakup cross-section of ^{6}Li and ^{7}Be has obviously confirmed the cluster structure of this nuclei, which was studied and established in [12].

For the case of ^{7}Be, the main reaction channels are ^{6}Li $+ p$ and ^{3}He $+$ ^{4}He as it is shown in Figure 6(b). The separation energies for these break-up channels are 5.606 MeV and 1.587 MeV respectively. The cross section values, therefore, are correlated somehow with the separation energies.

The most interesting result has been observed for ^{8}B as in Figure 6(c). This nucleus has mostly broken into ^{7}Be and proton with a large value of p-removal cross section $(240 \pm 20$ mb). This fact is a strong indication of ^{7}Be as a core of ^{8}B surrounded by a weakly bound "halo" proton.

Additionally we have to note that although ^{4}He is a tightly bound nucleus, we clearly identify its break up products such as p, d, t and ^{3}He after one neutron emission (see Figure 4). In total, the breakup reaction cross section of ^{4}He into charged particles is less than 32 ± 20 mb.

The graph in Figure 7 illustrates the dependence of the breakup cross section on the separation energy of the produced fragment. The evident trend is that the break-up cross section increases while the the separation energy decreases.
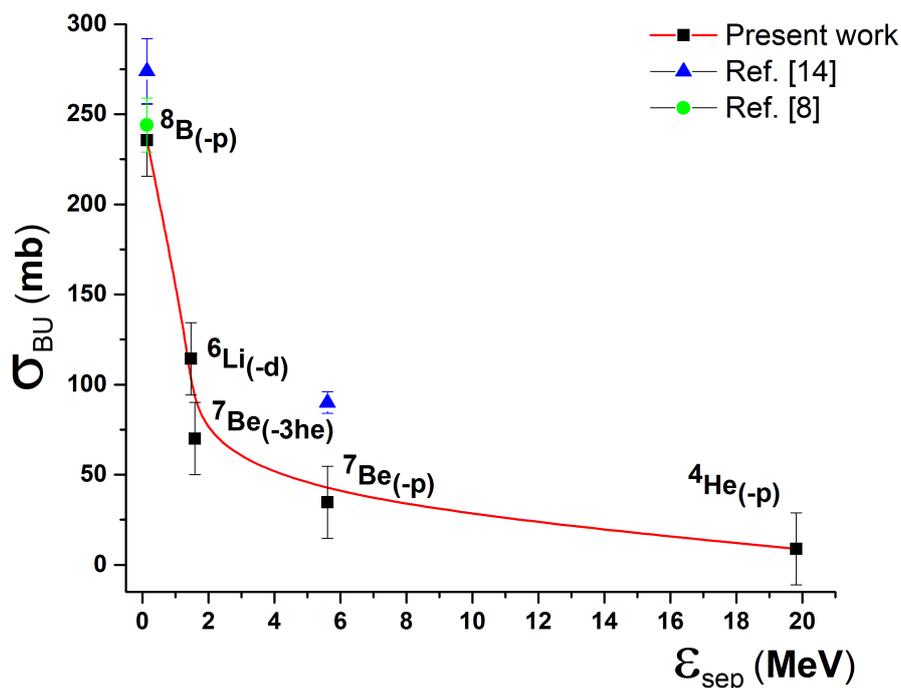

Figure 7. Dependence of the measured break-up cross section values for ^{4}He into triton, ^{6}Li into ^{4}He, ^{7}Be into ^{3}He and ^{8}B into ^{7}Be vs. respective separation energies.

Break-up momentum distribution.

Additionally to the break-up cross section measurement, the longitudinal momentum distributions of the selected breakup products of ^{6}Li, ^{7}Be and ^{8}B has been determined for the fifth detector taken as target.

Figure 8 shows: a) experimental momentum distribution for d and ^{3,4}He from break-up of ^{6}Li ions; b) experimental momentum distribution for d and ^{3,4}He and ^{6}Li from break-up of ^{7}Be ions; c) experimental momentum distribution for
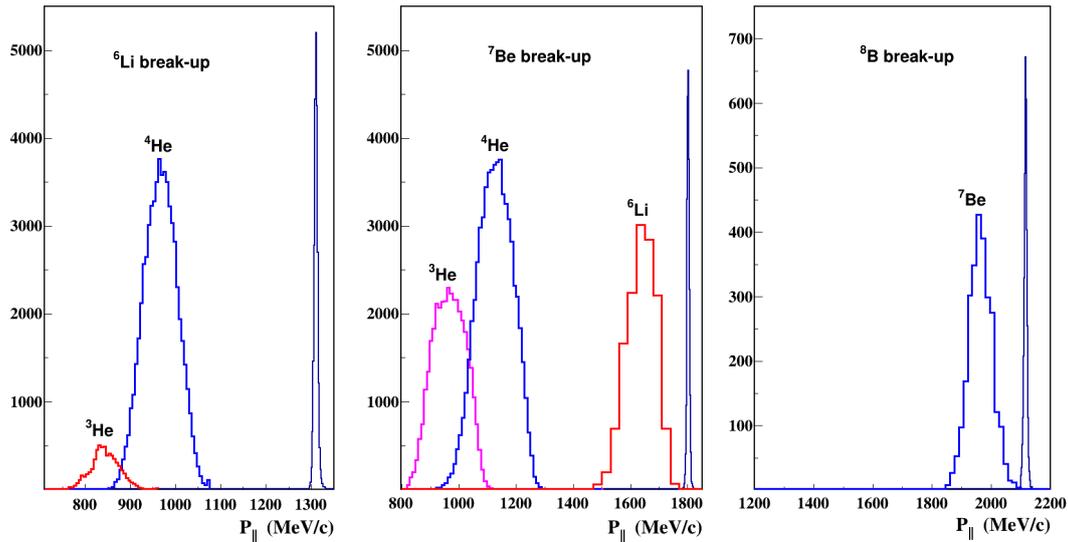
Figure 8.a) Experimental momentum distribution for d and ^{3,4}He from secondary beam of ^{6}Li ions b) experimental momentum distribution for d and ^{3,4}He and ^{6}Li from secondary beam of ^{7}Be ions and c) experimental momentum distribution for and ^{7}Be from secondary beam of ^{8}B ions.

^{7}Be from break-up of ^{8}B. Narrow peaks in the right side of the each insertion in Figure 8 correspond to the unreacted ^{6}Li, ^{7}Be and ^{8}B events. The experimental longitudinal momentum distribution was found from the non-reacted ^{6}Li, ^{7}Be and ^{8}B to be ~7 MeV/c (one standart deviation). The extracted full widths at half maximum (FWHM) of the measured longitudinal momentum distributions are listed in Table 1.

Perhaps the most striking features of the present experimental data are the large one proton-removal reaction cross-section for ^{8}B due to the small one proton separation energy (0.137 MeV) and the narrow momentum distribution of ^{7}Be fragment with full width at half maximum (FWHM) of 117 ± 12 MeV/c in good agreement with result in [8]. These findings support the existence of a one-proton halo in ^{8}B.

Table 1.
Momentum distributions of fragments resulting from fragmentation of ^{6}Li, ^{7}Be and ^{8}B

Projectile	E, A/MeV	Fragment	FWHM, MeV/c	Other work
^{6}Li	18	^{3}He	166 ± 11	
		^{4}He	103 ± 12	
^{7}Be	24	^{3}He	233 ± 12	
		^{4}He	172 ± 11	
		^{6}Li	196 ± 12	
^{8}B	30	^{7}Be	117 ± 10	93 ± 6 [8] 127 ± 17 [13]

Conclusion

In the present experiment,particle identification for secondary beam was performed by employing the Δ E-E method for a various isotope range from He to B isotopes. The Δ E and E were measured by the Si and CsI(Tl) telescope, respectively. Results on the break-up cross sections of some weakly bound light isotopes ^{6}Li, ^{7}Be and ^{8}B were obtained with a good statistic. The parallel momentum distribution of ^{3,4}He and ^{6}Li produced from the break-up of ^{6}Li, ^{7}Be and ^{8}B was also determined. Large one proton removal cross section for ^{8}B as well as narrow momentum distribution of ^{7}Be fragment confirm proton-halo structure of ^{8}B. We plan to carry out next experiment on total reaction cross-section, nucleon-removal cross section and elastic scattering measurements of other light neutron-rich nuclei using this technique and COMBAS fragment separator with improved statistics.

The fact that measurements of ^{8}B radius do not show a strong radius enhancement while breakup cross section and momentum distribution are in favour of the existence of a halo can be reconciled considering that the loosely bound proton in ^{8}B can be considered as a "confined halo" inside the Couloumb barier. In this case the wave function of the last proton is folded by the collisions with the walls of the Couloumb potential (reflections on the walls). This confinement refers only to the spatial extention of the halo, while other essential characteristic are preserved. It would be interesting to compare this situation with those of other nuclei canditates to proton halo, as it seems to be a general characteristic of this kind of nuclei. In their case, the "halo" attribute then becomes "confined halo".

Acknowledgments

References

[1] Yu.E. Penionzhkevich, Phys. Atom. Nucl. **72** (2009) 1617.
[2] I. Tanihata et al., Phys. Rev. Lett. **55** (1985) 2676.
[3] R. Warner et al., Phys. Rev. C **54** (1996) 1700 .
[4] T. Minamisono et al., Phys. Rev. Lett. **69** (1992) 2058.
[5] H. Nakada et al., Phys. Rev. C **49** (1994) 886.
[6] R. Warner et al., Phys. Rev. C **52** (1995) R1166.
[7] I. Tanihata et al., Phys. Rev. Lett. **206** (1988) 592.
[8] F. Negoita et al., Phys. Rev. C **54** (1996) 1787.
[9] C. Borcea et al., Nucl. Phys. A **616** (1997) 231.
[10] I. Pecina et al., Phys. Rev. C **52** (1995) 191.
[11] A. Artukh et al., Nucl. Inst. Meth. Phys. Res. A **426** (1999) 605.
[12] Y. Kanada-En'yo et al., Phys. Rev. C **52** (1995) 628.
[13] S.L. Jin et al., Phys. Rev. C **91** (2015) 054617.

[14] R. Warner et al., Phys. Rev. C **74** (2006) 014605.